Constant rate natural gas production from a well in a hydrate reservoir

Chuang Ji [a], Goodarz Ahmadi [a,*], Duane H. Smith [b]

[a] *Department of Mechanical and Aeronautical Engineering, Clarkson University, Potsdam, NY 13699-5725, USA*
[b] *National Energy Technology Laboratory, Department of Energy, Morgantown, WV 26507-0880, USA*

Abstract

Using a computational model, production of natural gas at a constant rate from a well that is drilled into a confined methane hydrate reservoir is studied. It is assumed that the pores in the reservoir are partially saturated with hydrate. A linearized model for an axisymmetric condition with a fixed well output is used in the analysis. For different reservoir temperatures and various well outputs, time evolutions of temperature and pressure profiles, as well as the gas flow rate in the hydrate zone and the gas region, are evaluated. The distance of the decomposition front from the well as a function of time is also computed. It is shown that to maintain a constant natural gas production rate, the well pressure must be decreased with time. A constant low production rate can be sustained for a long duration of time, but a high production rate demands unrealistically low pressure at the well after a relatively short production time. The simulation results show that the process of natural gas production in a hydrate reservoir is a sensitive function of reservoir temperature and hydrate zone permeability.

Keywords: Methane hydrate; Natural gas production; Hydrate dissociation; Computer model

1. Introduction

World reserves of natural gas hydrate have been estimated to be the largest fossil fuel resource among the known reserves of conventional natural gas and oil [11]. Thus, developing methods for commercial production of natural gas from hydrates has enormous economical and strategic importance.

Nomenclature

a, b, c	empirical constants in Eq. (4)
a	0.0342 K^{-1}
b	0.0005 K^{-2}
c	6.4804
a_n	thermal diffusivity of zones (m^2/s)
c_v	volume heat capacity of gas (3000 J/K kg)
c_1	heat capacity of zone 1 (2400.2 J/K kg)
c_2	heat capacity of zone 2 (1030.2 J/K kg)
k_1	phase permeability of gas in zone 1 (5.2 md)
k_2	phase permeability of gas in zone 2 (0.4 md)
r_0	radius of well
t	time
v_1	velocity of natural gas in zone 1
v_2	velocity of natural gas in zone 2
r	distance
z	compressibility of gas (0.88)
P_0	atmospheric pressure (1.01×10^5 Pa)
P_D	hydrate decomposition pressure
P_e	reservoir pressure at initial time (15 MPa)
P_G	pressure at well (MPa)
P_n	pressure in zone 1 or 2
Q	production rate of methane gas per unit length of well
R	radius of decomposition front
T_D	hydrate decomposition temperature (K)
T_e	reservoir temperature at initial time (K)
T_n	temperature in zone 1 or 2
T_0	273.15 K
α	water content of pores (0.15)
β	hydrate saturation of a layer (0.19)
γ	constant which determines movement velocity of dissociation front
δ	throttling coefficient of gas (8×10^{-7} K/Pa)
ε	mass fraction of gas in methane hydrate (0.129)
η	adiabatic coefficient of gas (3.2×10^{-6} K/Pa)
ρ_0	density of methane gas at atmospheric pressure P_0 and temperature T_0. (0.706 kg/m^3)
ρ_3	density of hydrate (0.91×10^3 kg/m^3)
ρ_W	density of water (1.0×10^3 kg/m^3)
μ	viscosity of gas (methane) (1.5×10^{-5} Pa s)
Φ	porosity (0.2)
Φ_1	$(1-\alpha)\Phi$, content of free gas at zone 1
Φ_2	$(1-\beta)\Phi$, content of free gas at zone 2

Natural gas hydrates are solid molecular compounds of water with natural gas that are formed under certain thermodynamically favorable conditions. The hydrate dissociates when its temperature increases to above the temperature of hydrate formation at a specified pressure, or when the system pressure decreases to below the pressure of hydrate formation at a specified temperature. When a well is drilled into a hydrate reservoir, it initiates a depressurization that leads to decomposition of hydrate and release of natural gas.

Makogon [11] and Sloan [15] provided extensive reviews of hydrate formation and decomposition processes. The hydrate decomposition process by depressurization has been studied by a number of authors. It is normally assumed that the process of hydrate decomposition by a pressure decrease is analogous to the process of solid melting. Makogon [10,11] used the classical Stefan's problem for melting to describe the process of hydrate decomposition. Verigin et al. [18] included the effect of gas and water mass balances at the decomposition front, but neglected the temperature variation of the hydrate layer during the movement of natural gas. Using the heat conduction equation, Holder et al. [5] included the variation of temperature during the hydrate decomposition in their study. Burshears et al. [3] extended the model of Holder et al. [5] and considered the influence of water transport in the layer, in addition to the natural gas flow. Selim and Sloan [16] obtained an analytical expression for the temperature distribution in the reservoir using the convection heat transfer equation in their one dimensional model. Kamath [7] experimentally studied the process of hydrate dissociation using hot water. He also used a modified Clausius–Clapeyron equation to obtain the enthalpy of dissociation for hydrates of different gases. Recent studies on geological aspects of hydrates were reported in the American Geophysical Union [1].

The study of Bondarev and Cherskiy, where the effects of heat transfer in the porous medium were included, was summarized by Makogon [11]. The energy equation was used to describe the thermal condition of natural gas in the porous layer. The conductive–convective heat transfer and effects of the throttling process were included. Makogon [11] also reported the linearized governing equations and the corresponding analytical expressions for the one dimensional and axisymmetric temperature and pressure profiles.

Lysne [9] discussed the water and gas flow during the dissociation of hydrate in a pipe. He showed an axisymmetric pressure distribution in the pipe numerically. Tsypkin [17] also described the movement of water and gas in the reservoir using a multiphase one dimensional model. He obtained similarity solutions for the temperature and pressure distributions by a perturbation method. Masuda et al. [13] treated the process of hydrate dissociation as a Kim–Bishnoi [8] kinetic process. In this model, the rate of dissociation is related to the difference between the equilibrium pressure and gas pressure. Their numerical results were in agreement with their experimental data.

Moridis et al. [14] added a module for hydrate dissociation into the TOUGH2 general purpose reservoir simulator. The flows of gas and water were considered and the conductive–convective heat transfer equation was used. Hydrate dissociation by injection of hot water into the reservoir was studied by Durgut and Parlaktuna [4]. A two dimensional model, which included the heat conduction and convection and water and gas flows, was used in this study. Ahmadi et al. [2] and Ji et al. [6] studied natural gas production from hydrate reservoirs using a Cartesian one dimensional numerical model.

The present study is concerned with the problem of natural gas production with constant well output from a hydrate reservoir. The case that the reservoir is partially saturated with hydrate and

the reservoir contains pressurized natural gas is considered. The linearized form of the governing equations as reported by Makogon [11] is used in the analysis. The special case that a well is drilled in an unbounded axisymmetric hydrate reservoir is studied. When the well output is at a fixed rate, a set of self-similar solutions for the temperature and pressure distributions in the reservoir can be found. The approach leads to a system of coupled algebraic equations for the location of the decomposition front and the temperature and pressure at the front. This system of equations is then solved by an iterative scheme. Numerical results for time evolutions of the pressure and temperature profiles in the hydrate reservoir, as well as the location of the front, are obtained for several well natural gas production rates and reservoir temperatures. The simulation results are presented in graphical form and discussed.

2. Hydrate decomposition model

Natural gas production from dissociation of methane hydrate in an unbounded axisymmetric reservoir due to drilling of a depressurization well is studied. The reaction of methane with water to form hydrate is represented by

$$(CH_4)_{gas} + 6(H_2O)_{water} \leftrightarrow (CH_4 \cdot 6H_2O)_{solid}$$

Under thermodynamically favorable conditions, the water molecules form a cage around the methane molecule and form the solid hydrates. When the pressure decreases or the temperature rises, the reaction reverses and the hydrate decomposes into CH_4 and water.

Consider an unbounded methane hydrate reservoir underground that is partially saturated with solid hydrate and also contains pressurized natural gas at the reservoir pressure P_e and reservoir temperature T_e. At this reservoir pressure, the hydrate must be stable, with $P_e > P_D$, where P_D is the hydrate dissociation pressure at dissociation temperature T_D. When a well is drilled into the reservoir, the pressure in the well drops to a certain value less than $P_D < P_e$. The hydrate near the well becomes unstable and dissociates into natural gas and water. The process of hydrate dissociation then expands radially outward from the well with time. It is believed that the hydrate dissociation occurs in a narrow region, which can be treated as the dissociation front. This moving cylindrical front separates the volume of the reservoir into two zones with different phases. The near well gas zone contains natural gas and liquid water, while the hydrate zone beyond the dissociation front contains the solid hydrate and natural gas. Pressures and temperatures in these two zones gradually decrease as the natural gas flows towards the well, while the dissociation front moves away from the well.

In this analysis, it is assumed that the hydrate reservoir contains natural gas (i.e. it is not a solid chunk of hydrate). The heat needed for hydrate dissociation is supplied by the flow of gas from the hydrate zone to the decomposition front. The pressure and temperature at the dissociation front are the equilibrium pressure, P_D, and temperature, T_D. The temperature and pressure distributions are axiasymmetric with respect to the well centerline. The decomposition front is also a cylinder with its axis at the well.

3. Mathematical model

In this section, the mathematical formulations proposed by Makogon [11] for evaluation of the pressure and temperature fields are summarized.

Consider a hydrate reservoir with a fixed production rate depressurizing well as shown in Fig. 1. The governing equation for the pressure distribution in the reservoir, which is obtained from the continuity equation and Darcy's law, is given as

$$\frac{k_n}{2\Phi_n\mu}\left(\frac{\partial^2 P_n^2}{\partial r^2}+\frac{1}{r}\frac{\partial P_n^2}{\partial r}\right)=\frac{\partial P_n}{\partial t} \tag{1}$$

where

$$\Phi_1=(1-\alpha)\Phi \tag{2}$$

$$\Phi_2=(1-\beta)\Phi \tag{3}$$

and r is the radial distance from the well, t is time, μ is the coefficient of viscosity of the gas, k_n is the gas permeability in zone 1 or 2, P_n is the pressure in zone 1 or 2, Φ is the reservoir porosity, α is the water saturation and β is the hydrate saturation. In Eq. (1) and in the subsequent analysis, $n=1$ corresponds to the gas region with $r_0<r<R(t)$, and $n=2$ denotes the hydrate region with $R(t)<r<\infty$. Here, $R(t)$ is the distance of the dissociation front from the center of the well, and r_0 is the well radius.

The relation between dissociation temperature T_D and pressure P_D at the decomposition front for phase equilibrium between natural gas and hydrate is given as

$$\log_{10} P_D=a(T_D-T_0)+b(T_D-T_0)^2+c \tag{4}$$

where T_0 is 273.15 K and a, b and c are empirical constants that depend on the hydrate composition. Values of a, b, and c are obtained using the least square error fit to the equilibrium pressure–temperature data for methane hydrate [6,11], i.e.

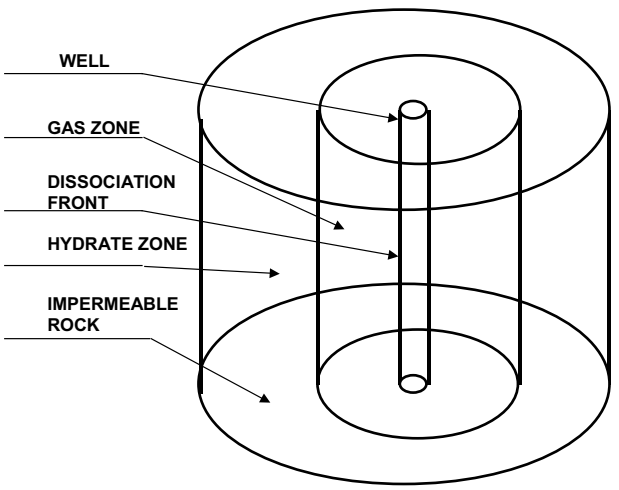

Fig. 1. Schematic of an axisymmetric hydrate reservoir.

$$a = 0.0342\ \mathrm{K}^{-1}, \qquad b = 0.0005\ \mathrm{K}^{-2}, \qquad c = 6.4804$$

where, in Eq. (4), P_D is in Pa.

Ji et al. [6] showed that the prediction of Eq. (4) is in good agreement with the data of Marshal et al. [12]. The mass balance for gas at the decomposition front at the distance of $R(t)$ from the well is given as [18]

$$\rho_1 \upsilon_1 - \rho_2 \upsilon_2 = -[\beta\varepsilon\rho_3 - (1-\alpha)\rho_1 + (1-\beta)\rho_2]\Phi\frac{\mathrm{d}R}{\mathrm{d}t} \tag{5}$$

where ρ_1 is the density of natural gas in zone 1, ρ_2 is the density of natural gas in zone 2, ρ_3 is the density of hydrate and ε is the mass fraction of methane gas in the hydrate. Here, υ_1 and υ_2 are, respectively, the velocities of natural gas at the dissociation front in zones 1 and 2.

The densities of the natural gas in zones 1 and 2 at the dissociation front are described by the same equation:

$$\rho_1(R,t) = \rho_2(R,t) = \rho_0\frac{P_D T_0}{z P_0 T_D} \tag{6}$$

where z is the gas compressibility (deviation) factor and ρ_0 is the gas density at standard pressure P_0 and temperature T_0. Insertion of Eq. (6) into Eq. (5) gives

$$\upsilon_1(R,t) - \upsilon_2(R,t) = -\left[\varepsilon\beta\frac{\rho_3 P_0 T_D}{\rho_0 P_D T_0} z - (\beta-\alpha)\right]\Phi\frac{\mathrm{d}R}{\mathrm{d}t} \tag{7}$$

Similarly, the mass balance equation for water is:

$$\rho_W \Phi\alpha = (1-\varepsilon)\rho_3\Phi\beta \tag{8}$$

where ρ_W is the density of water.

The temperature field is governed by the convective–conductive heat transfer equation

$$\frac{a_n}{r}\frac{\partial}{\partial r}\left(r\frac{\partial T_n}{\partial r}\right) = \frac{\partial T_n}{\partial t} - \frac{c_v k_n}{c_n \mu}\frac{\partial P_n}{\partial r}\left(\frac{\partial T_n}{\partial r} - \delta\frac{\partial P_n}{\partial r}\right) - \eta\frac{\Phi_n c_v}{c_n}\frac{\partial P_n}{\partial t} \tag{9}$$

Here, a_n is the heat diffusivity, c_n is the heat capacity, c_v is the constant volume heat capacity of gas, δ is the throttling coefficient and η is the adiabatic coefficient of the gas. Note that the Joule–Thompson throttling process is taken into account in Eq. (9).

For wells with a fixed natural gas output, Q, the boundary conditions are

$$Q = 2\pi r_0 h\frac{k_1}{\mu}\left[\rho\frac{\partial P_1}{\partial r}\right]_{r=r_0} = \frac{\pi k_1 h}{\mu}\frac{\rho_0}{P_0}\left[r\frac{\partial P_1^2}{\partial r}\right]_{r=r_0} = \frac{\pi k_1 h}{\mu}\frac{\rho_0}{P_0}c_1 \tag{10}$$

$$P_2(r,0) = P_2(\infty,t) = P_e \tag{11}$$

$$P_1(R(t),t) = P_2(R(t),t) = P_D(T_D) \tag{12}$$

$$T_2(r,0) = T_2(\infty,t) = T_e \tag{13}$$

$$T_1(R(t),t) = T_2(R(t),t) = T_D \tag{14}$$

where h is the thickness of the hydrate reservoir and c_1 is a constant (related to the pressure gradient at the well wall). As noted before, it is assumed that the dissociation front is at the equilibrium pressure and temperature (P_D and T_D) for dissociation of the hydrate.

4. Linearization and self-similar solution

To be able to obtain similar solutions, Eq. (1) must be first linearized. Here, the reservoir and the dissociation pressures are, respectively, used to linearize the pressure equation in the hydrate and gas zones. That is, using the approximation

$$\frac{\partial P_1^2}{\partial t} \approx 2P_D \frac{\partial \overline{P}_1}{\partial t} \qquad \frac{\partial P_2^2}{\partial t} \approx 2P_e \frac{\partial \overline{P}_2}{\partial t} \tag{15}$$

Eq. (1) may be linearized as:

$$\frac{\partial \overline{P}_n^2}{\partial r^2} + \frac{1}{r}\frac{\partial \overline{P}_n^2}{\partial r} = \frac{1}{\chi_n}\frac{\partial \overline{P}_n^2}{\partial t} \tag{16}$$

where

$$\chi_1 = \frac{k_1 P_D}{\mu \Phi_1} \qquad \chi_2 = \frac{k_2 P_e}{\mu \Phi_2} \tag{17}$$

Self-similar solutions of Eq. (16) with boundary conditions (10)–(14) are:

$$\overline{P}_1^2 = P_D^2 - \frac{Q\mu}{2\pi k_1 h}\frac{P_0}{\rho_0}\left[E_i\left(-\lambda_1^2\right) - E_i\left(-\alpha_1^2\right)\right] \tag{18}$$

$$\overline{P}_2^2 = P_e^2 - (P_e^2 - P_D^2)\frac{E_i(-\lambda_2^2)}{E_i(-\alpha_2^2)} \tag{19}$$

where

$$E_i(-\xi) = -\int_{\xi}^{\infty} \frac{e^{-u}}{u}\,du \tag{20}$$

$$\lambda_1 = \frac{r}{2\sqrt{\chi_1 t}} \qquad \lambda_2 = \frac{r}{2\sqrt{\chi_2 t}} \tag{21}$$

$$\alpha_1 = \sqrt{\frac{\gamma}{4\chi_1}} \qquad \alpha_2 = \sqrt{\frac{\gamma}{4\chi_2}} \tag{22}$$

Under the condition that the hydrate reservoir contains free natural gas, neglecting the conductive heat transfer in the porous media, which is several orders of magnitude smaller than the convective heat transfer, Eq. (9) becomes

$$\frac{\partial T_n}{\partial t} = \frac{c_v k_n}{c_n \mu}\frac{\partial P_n}{\partial r}\left(\frac{\partial T_n}{\partial r} - \delta\frac{\partial P_n}{\partial r}\right) + \eta\frac{\Phi_n c_v}{c_n}\frac{\partial P_n}{\partial t} \tag{23}$$

Similarly, solutions to the linearized form of Eq. (23) satisfying the boundary conditions (10)–(14) are:

$$T_1 = T_D + A_1\delta\left[E_i(-\lambda_1^2) - E_i(-\alpha_1^2) + \left(\frac{\eta}{\delta}B_1 - 1\right)(\Psi_1(\lambda_1^2) - \Psi_1(\alpha_1^2))\right] \tag{24}$$

$$T_2 = T_e + A_2\delta\left[E_i(-\lambda_2^2) - \left(\frac{\eta}{\delta}B_2 - 1\right)\Psi_2(\lambda_2^2)\right] \tag{25}$$

where

$$\Psi_1(\xi) = \int_0^{\xi} \frac{e^{-\eta}}{\eta + C_1 e^{-\eta}}\,d\eta \qquad \Psi_2(\xi) = \int_{\xi}^{\infty} \frac{e^{-\eta}}{\eta + C_2 e^{-\eta}}\,d\eta \tag{26}$$

$$A_1 = \frac{Q\mu P_0}{4\pi P_D k_1 \rho_0 h}; \qquad A_2 = -\frac{1}{2E_i(-\alpha_2^2)}\frac{P_e^2 - P_D^2}{P_e} \tag{27}$$

$$B_1 = \frac{\Phi_1 c_v}{c_1} \qquad B_2 = \frac{\Phi_2 c_v}{c_2} \tag{28}$$

$$C_1 = \frac{Qc_v P_0}{4\pi P_D c_1 \chi_1 h \rho_0}; \qquad C_2 = -\frac{P_e^2 - P_D^2}{P_e}\frac{c_v}{c_2}\frac{1}{2E_i(-\alpha_2^2)}\frac{k_2}{\mu\chi_2} \tag{29}$$

The values of pressure P_D and temperature T_D at the dissociation front and the constant γ, which determines the motion of the decomposition front, are still unknown and must be evaluated numerically for a given set of conditions. From the evaluation of Eq. (25) at the decomposition front (i.e. $\lambda_2 = \alpha_2$), it follows that:

$$T_D = T_e + A_2\delta\left[E_i(-\alpha_2^2) - \left(\frac{\eta}{\delta}B_2 - 1\right)\Psi_2(\alpha_2^2)\right] \tag{30}$$

The equilibrium pressure P_D and the equilibrium temperature T_D are related through Eq. (7). Substituting Eqs. (18) and (19) into Eq. (4), we obtain the equation for determining the constant γ, i.e.

$$Q\frac{P_0}{\pi}\frac{e^{-\alpha_1^2}}{h\rho_0} + \frac{2k_2}{\mu}(P_e^2 - P_D^2)\frac{e^{-\alpha_2^2}}{E_i(-\alpha_2^2)} = A\gamma \tag{31}$$

where

$$A = \left[\varepsilon\beta\frac{\rho_3 P_0 T_D}{\rho_0 T_0}z - (\beta - \alpha)P_D\right]\Phi \tag{32}$$

Eqs. (4), (30) and (31) are three nonlinear coupled equations for determining γ, T_D and P_D.

The linearization model described in this section that was suggested by Makogon [11] assumes that the heat convection dominates the conduction and he neglects the heat conduction in the entire reservoir. While this assumption is reasonable away from the dissociation front, it does not allow for the energy balance at the dissociation front to be enforced. Despite this important limitation of the approach, the linearization method provides a convenient (semi-analytical) means for studying many features of the natural gas production from hydrate reservoirs.

5. Results

In this section, the results for the time evolution of the pressure and temperature profiles in the hydrate reservoir due to the presence of a well with different fixed natural gas outputs are presented. In addition, the time variations of location of the dissociation front are also evaluated. The conditions listed in the nomenclature and an initial reservoir pressure of 15 MPa are used in these simulations. For different values of well output and initial reservoir temperatures, the solutions to Eqs. (4), (30) and (31) are obtained. The resulting values of the dissociation temperature and pressure at the front and of the parameter γ (with an error bound of 0.1%) are listed in Table 1. Here, the permeability in the gas zone is 5.2 md, and the hydrate zone permeability is 0.4 md.

When the reservoir pressure, temperature and production rates are specified, the present linearized axisymmetric model leads to fixed values of dissociation front pressure and temperature. The well pressure, however, changes gradually with time. Table 1 shows that for a fixed reservoir temperature of 287 K, when the natural gas output decreases, the dissociation pressure and temperature decrease slightly. The value of parameter γ, which controls the movement of the dissociation front, however, decreases sharply as the gas production decreases. The dissociation pressure and temperature are sensitive functions of reservoir temperature. When the gas production is kept fixed at 0.03 kg/s, a decrease of 2 K in the reservoir temperature drops the dissociation pressure by about 17%. In this case, parameter γ also decreases with the decline of reservoir temperature.

For a reservoir temperature of 287 K and a natural gas production rate of 0.04 kg/s, variations of the decomposition temperature and pressure and parameter γ with zone permeability are shown in Table 2. When the permeability in the gas zone is fixed at 5.2 md, as the hydrate zone

Table 1
Values of dissociation temperature and pressure and parameter γ for different natural gas production rates for a reservoir with $k_1 = 5.2$ md and $k_2 = 0.4$ md

P_e (MPa)	T_e (K)	Natural gas output (kg/s)	T_D (K)	P_D (MPa)	γ (m^2/s)
15	283	0.03	277.25	4.314	1.61×10^{-6}
15	285	0.03	279.46	5.526	2.45×10^{-6}
15	287	0.04	281.96	6.65	2.71×10^{-5}
15	287	0.03	281.96	6.647	4.67×10^{-6}
15	287	0.02	281.93	6.628	1.4×10^{-7}
15	287	0.01	281.92	6.61	2.51×10^{-8}

Table 2
Values of dissociating temperature and pressure and parameter γ for a natural gas production rate of 0.04 kg/s for different zone permeabilities

P_e (MPa)	Permeability of gas zone (md)	Permeability of Hydrate zone (md)	T_D (K)	P_D (MPa)	γ (m^2/s)
15	5.2	3	282.038	6.7	4.96×10^{-10}
15	5.2	1	281.976	6.66	2.5×10^{-8}
15	5.2	0.6	281.964	6.65	2.9×10^{-6}
15	5.2	0.4	281.963	6.65	2.71×10^{-5}
15	1	1	281.978	6.66	2.51×10^{-8}

permeability decreases from 3 to 0.4 md, the dissociation pressure and temperature decrease slightly, while parameter increases sharply. This is because, when the hydrate zone permeability is low, the amount of hydrate that needs to dissociate increases to maintain the well gas flow at a fixed rate. When the permeability in the hydrate zone is fixed, variations of the gas zone permeability have a very slight effect on the dissociation temperature, pressure and parameter γ. As noted before, here, the natural gas output is fixed, and therefore, the equilibrium conditions at the front do not change appreciably. The main effect of variations of gas zone permeability is on the temperature and pressure profiles, which will be discussed later.

For a reservoir temperature of 287 K and a natural gas production rate of 0.04 kg/s, Fig. 2 shows variations of the pressure and temperature profiles at different times. Here, the permeability in the hydrate and gas zones are, respectively, 5.2 and 0.4 md. As noted before, the hydrate reservoir is divided into two zones by the dissociation front, and the temperature variations in the two zones are quite different. Fig. 2a and b show that the temperature decreases gradually from the undisturbed reservoir value far from the front to the dissociation temperature at the front. In the gas zone, the temperature varies gradually near the dissociation front but decreases sharply to its minimum values at the well. The temperature profiles in the hydrate and the gas zones are also self-similar and evolve with time as the decomposition front moves outward.

The corresponding pressure profiles for different times under the same conditions for the far and near fields are presented in Fig. 2c and d. The pressure decreases gradually from the reservoir

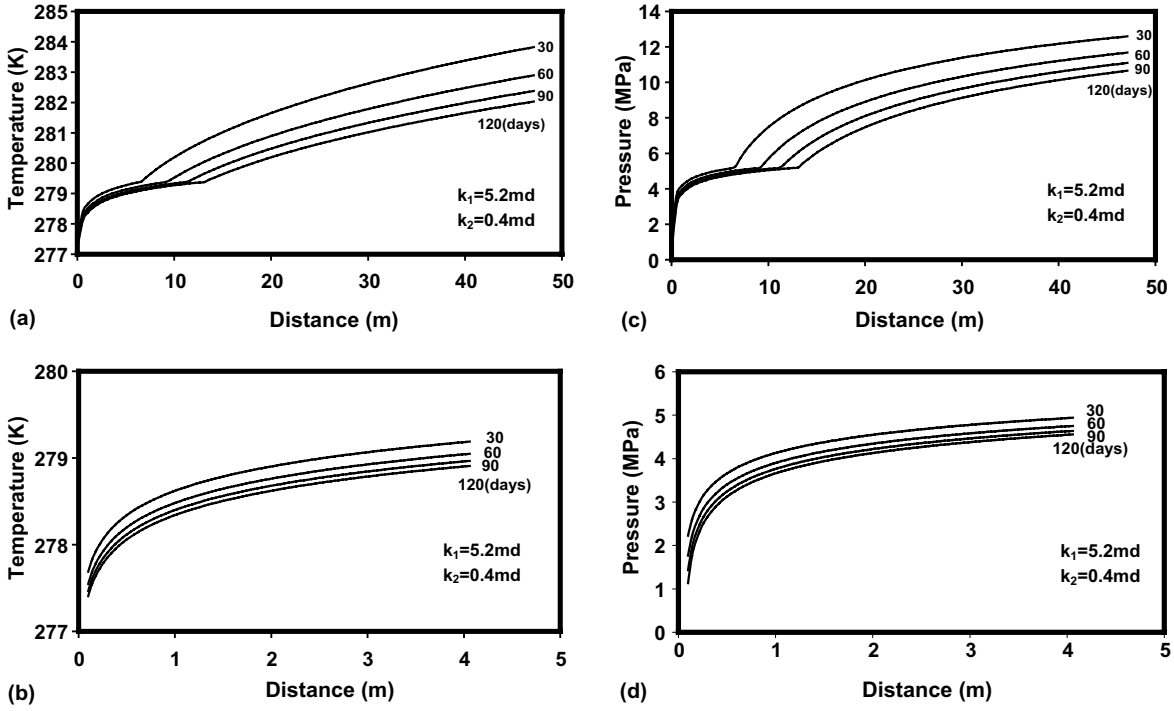

Fig. 2. Time variations of pressure and temperature profiles for a reservoir temperature of 287 K and a well natural gas output of 0.04 kg/s. (a), (c) extended field. (b), (d) near-well.

pressure to the dissociation pressure at the front and then decreases toward the well to its minimum value at the well. Near the well, the pressure gradient becomes quite high.

For the present case, where the permeability of the gas zone is thirteen times that of the hydrate zone, the change in the slope of the pressure profile at the dissociation front can be clearly seen from Fig. 2c. This is quite different from the one dimensional model of Ji et al. [6], in which the gradient change at the front was hardly noticeable. It should be emphasized that in the earlier study of Ji et al. [6], the permeability in the gas zone was almost the same as that in the hydrate zone. Fig. 2c also shows that the pressure profiles for different times are self-similar in each zone and expand outward as the dissociation front moves away from the well.

Fig. 2d shows that the pressure at the well drops with time when the natural gas output is kept fixed (at 0.04 kg/s). That is, to maintain a constant gas output, the well pressure must be reduced continuously with time. Obviously, this can not continue forever, and after a certain time, the pressure at the well becomes too low to allow maintaining a constant flow rate.

For a natural gas production rate of 0.04 kg/s, the time evolutions of the gas mass flux (ρv) and the total mass flow ($2\pi r\rho v$) across the reservoir are displayed, respectively, in Fig. 3a and b. Fig. 3a shows that the gas mass flux increases toward the well, and the variation in each zone is roughly time independent. This figure also clearly shows the details of natural gas production at the dissociation front. At the front, there is a jump in the mass flux due to the hydrate dissociation. The jump moves outward with time as the dissociation front penetrates deeper into the hydrate reservoir.

Fig. 3b shows the time variation of the total mass flow at a radial distance of r from the well. The total mass flow profiles in the hydrate and the gas zones remain roughly fixed, except for the jump at the dissociation front. This figure clearly shows the variation of the amount of natural gas generated by hydrate dissociation at the front. There is also a slight decrease in the gas flow in the hydrate zone that is compensated by the slight increase in the gas production by dissociation at the front. Fig. 3a indicates that the mass flux due to hydrate dissociation decreases with time. On the other hand, Fig. 3b indicates that the total mass flow due to hydrate dissociation remains fixed (or increases slightly) with time.

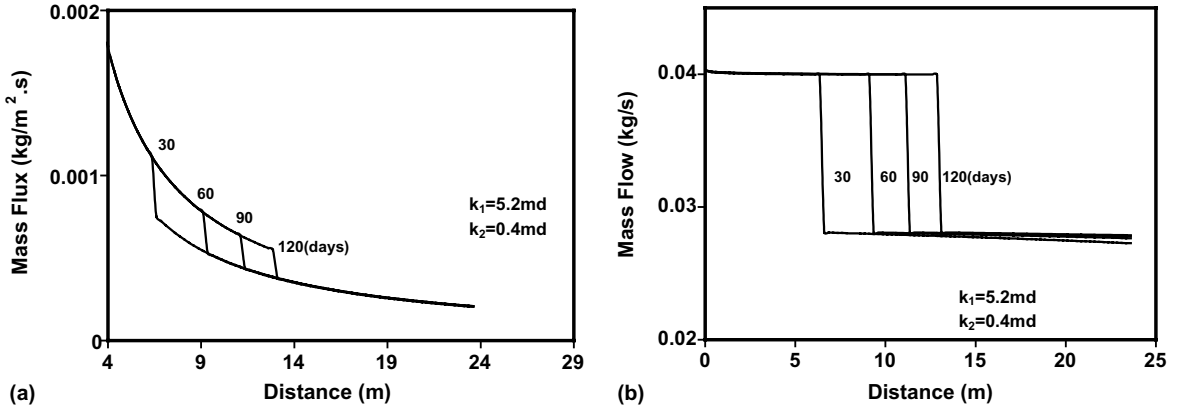

Fig. 3. Mass flux and total mass flow profiles for a reservoir temperature of 287 K and a well natural gas output of 0.04 kg/s.

Fig. 4 shows the pressure and temperature profiles for a natural gas production rate of 0.03 kg/s in a reservoir with permeabilities in the hydrate and gas zones being equal to 5.2 and 0.4 md. The reservoir pressure and temperature are kept constant at 15 MPa and 287 K. This figure shows that large pressure and temperature gradients occur near the front on the hydrate side. The pressure and temperature in the gas region then decrease gradually toward their minimum values at the well. The pressure and temperature profiles in the gas zone in Fig. 4 are similar to those shown in Fig. 2 with certain differences. In addition to the slower movement of the dissociation front for the lower well output in this case, the temperature and pressure gradients near the well become more gradual. Comparing Figs. 2d and 4d shows that the time variation of the well pressure also becomes much slower when the gas output decreases. This implies that a constant well output of 0.03 kg/s can be maintained for a much longer time period when compared to that of 0.04 kg/s.

The time evolutions of mass flux and total mass flow in the reservoir for a well output of 0.03 kg/s are shown in Fig. 5. Except for the lower magnitudes, the mass flux and the total mass flow profiles are quite similar to those shown in Fig. 3. The details of the hydrate dissociation at the front and the motion of the front can also be seen from this figure.

Under the same reservoir conditions, when the natural gas output is fixed at 0.02 kg/s, Fig. 6 shows that the dissociation front moves at a much slower rate. Other features of the pressure and temperature profiles in the hydrate zone are similar to those for higher well gas outputs. In this case, however, the pressure and temperature profiles in the hydrate zone have sharp gradients near the front. Fig. 6b and d show the details of the temperature and pressure profiles near the well. The temperature and pressure vary smoothly toward the well and decrease slightly with time. The

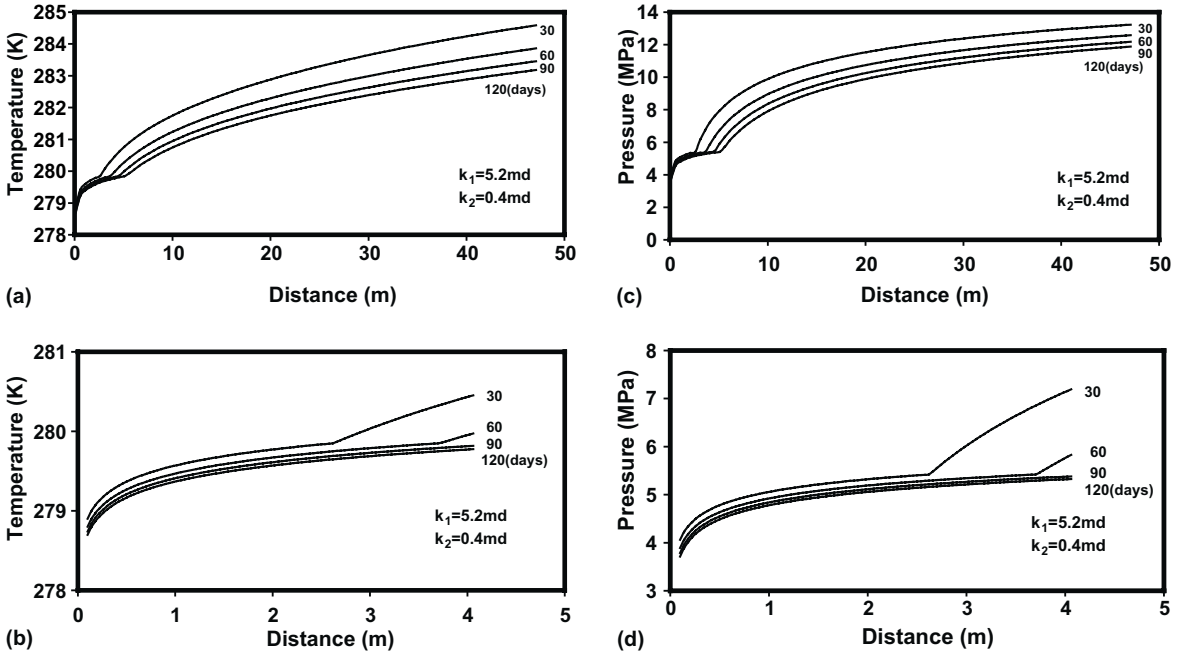

Fig. 4. Time variations of pressure and temperature profiles for a reservoir temperature of 287 K and a well natural gas output of 0.03 kg/s. (a), (c) extended field. (b), (d) near-well.

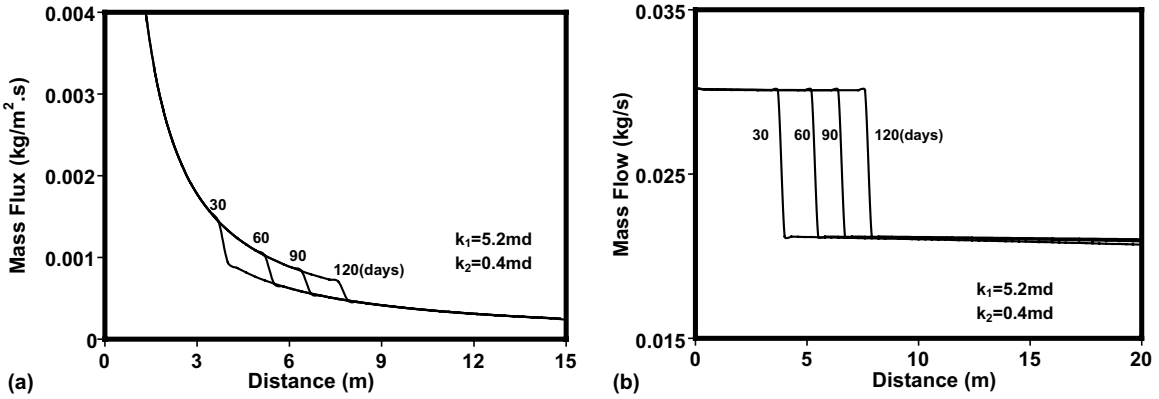

Fig. 5. Mass flux and total mass flow profiles for a reservoir temperature of 287 K and a well natural gas output of 0.03 kg/s.

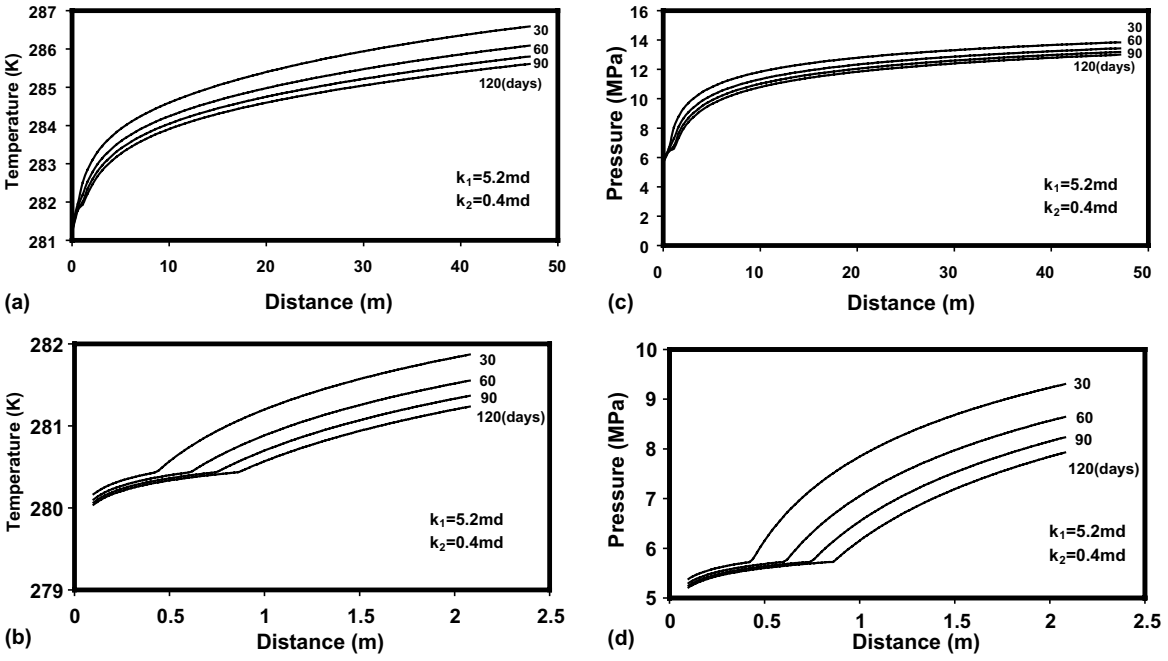

Fig. 6. Time variations of pressure and temperature profiles for a reservoir temperature of 287 K and a well natural gas output of 0.02 kg/s. (a), (c) extended field. (b), (d) near-well.

corresponding mass flux and mass flow profiles are shown in Fig. 7. The general features of these profiles are similar to those for higher well outputs. In this case, however, the dissociation front moves only a few meters after 120 days, but similar jumps in the mass flux and mass flow rate are observed.

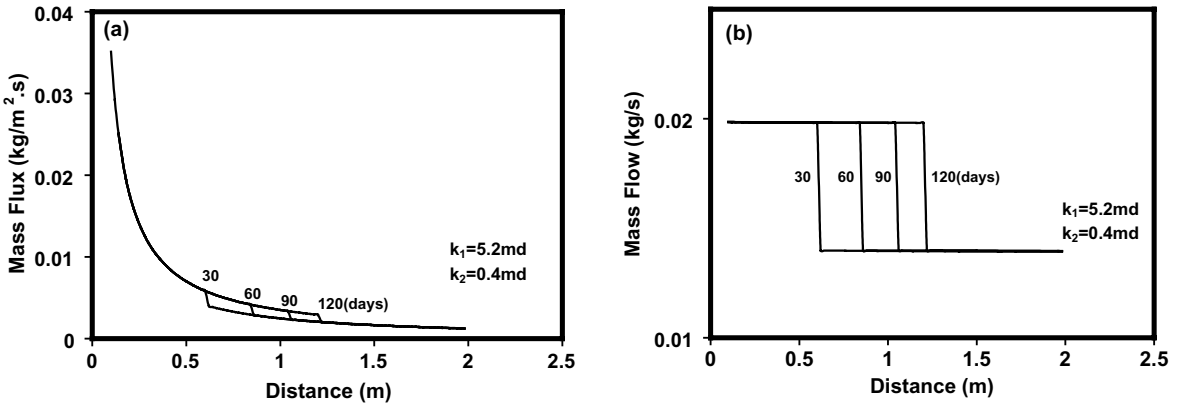

Fig. 7. Mass flux and total mass flow profiles for a reservoir temperature of 287 K and a well natural gas output of 0.02 kg/s.

For the case that the natural gas output is kept fixed at 0.03 kg/s, for a reservoir temperature of 285 K (2 K lower that the case shown in Fig. 4), the pressure and temperature profiles are presented in Fig. 8. The zone permeabilities are also kept the same. While the general features of the pressure and temperature profiles in Fig. 8 are similar to those shown in Fig. 4, the dissociation

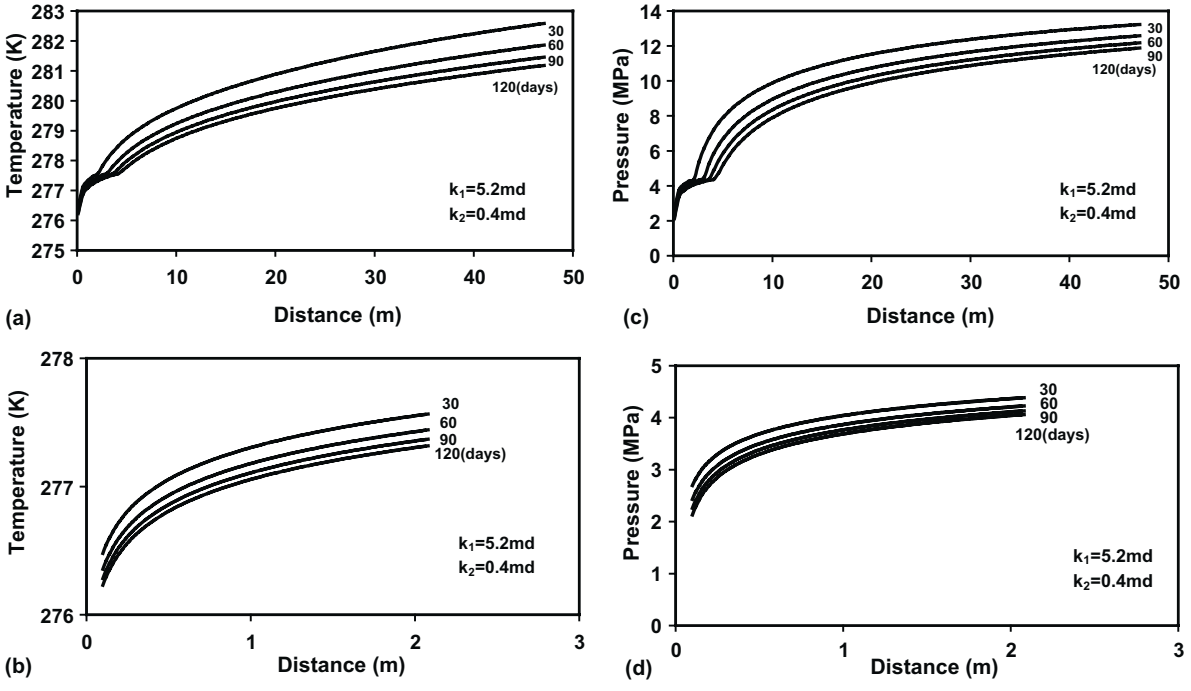

Fig. 8. Time variations of pressure and temperature profiles for a reservoir temperature of 285 K and a well natural gas output of 0.03 kg/s. (a), (c) extended field. (b), (d) near-well.

pressure and temperature at the front are somewhat smaller. The movement of the front has also noticeably slowed for this lower temperature reservoir. This observation further emphasizes the importance of heat transfer for the hydrate dissociation and natural gas production processes. In this axisymmetric model, the heat required for hydrate dissociation must be supplied by the hydrate reservoir. Therefore, the reservoir temperature becomes an important controlling parameter. It should be emphasized that for thin hydrate reservoirs, heat could also be supplied from the lower warmer region, which would significantly affect the natural gas production process.

Fig. 9 shows the temperature and pressure profiles when the reservoir temperature is 283 K, the other reservoir conditions being kept fixed, and the well output is 0.03 kg/s. Compared with Figs. 4 and 8, it is seen that the temperature and the pressure profiles are quite similar. However, due to the lower decomposition temperature and pressure, the rate of reduction of pressure at the well increases. In particular, Fig. 9d shows that the well pressure becomes too low at about 120 days to maintain a constant gas output of 0.03 kg/s. Therefore, as the reservoir temperature decreases, the time duration that a fixed natural gas output can be maintained becomes shorter.

Mass flux and mass flow profiles for reservoir temperatures of 283 and 285 K are compared in Fig. 10. While the mass flux jumps for different reservoir temperatures are comparable, the decomposition front moves faster when the reservoir temperature is higher. Comparing Figs. 5 and 10 shows the same trend of variations.

The effect of variations in zone permeability on the reservoir temperature and pressure profiles are shown in Fig. 11. Here, the case where the reservoir temperature is 287 K and the natural gas

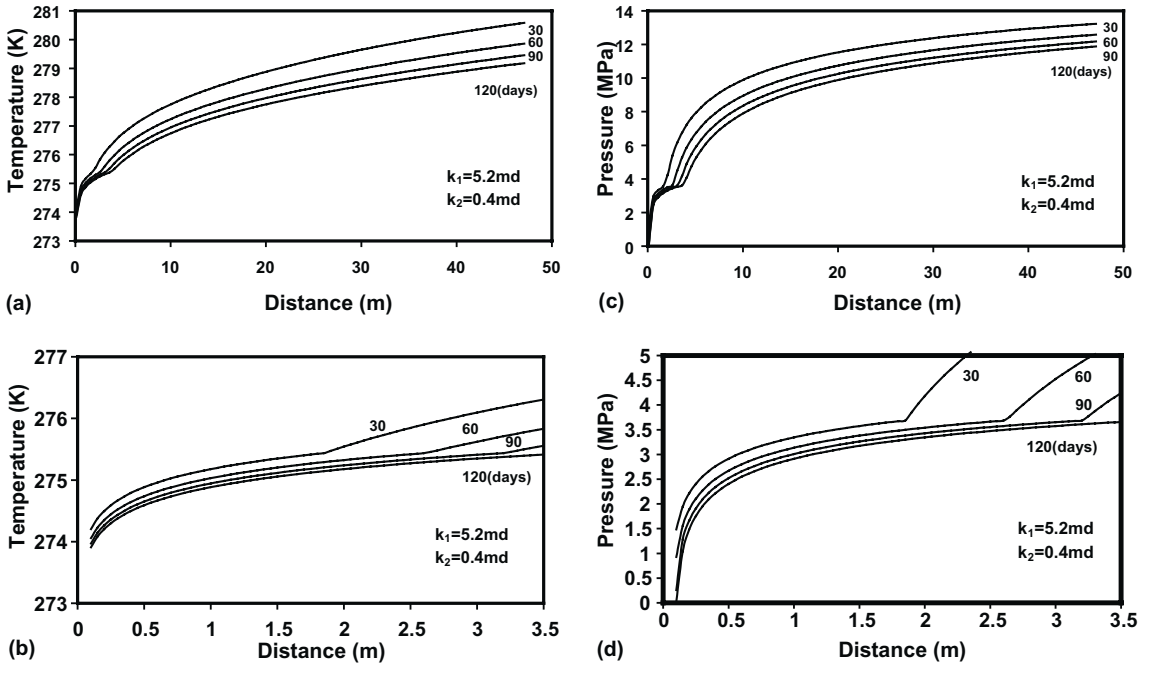

Fig. 9. Time variations of pressure and temperature profiles for a reservoir temperature of 283 K and a well natural gas output of 0.03 kg/s. (a), (c) extended field. (b), (d) near-well.

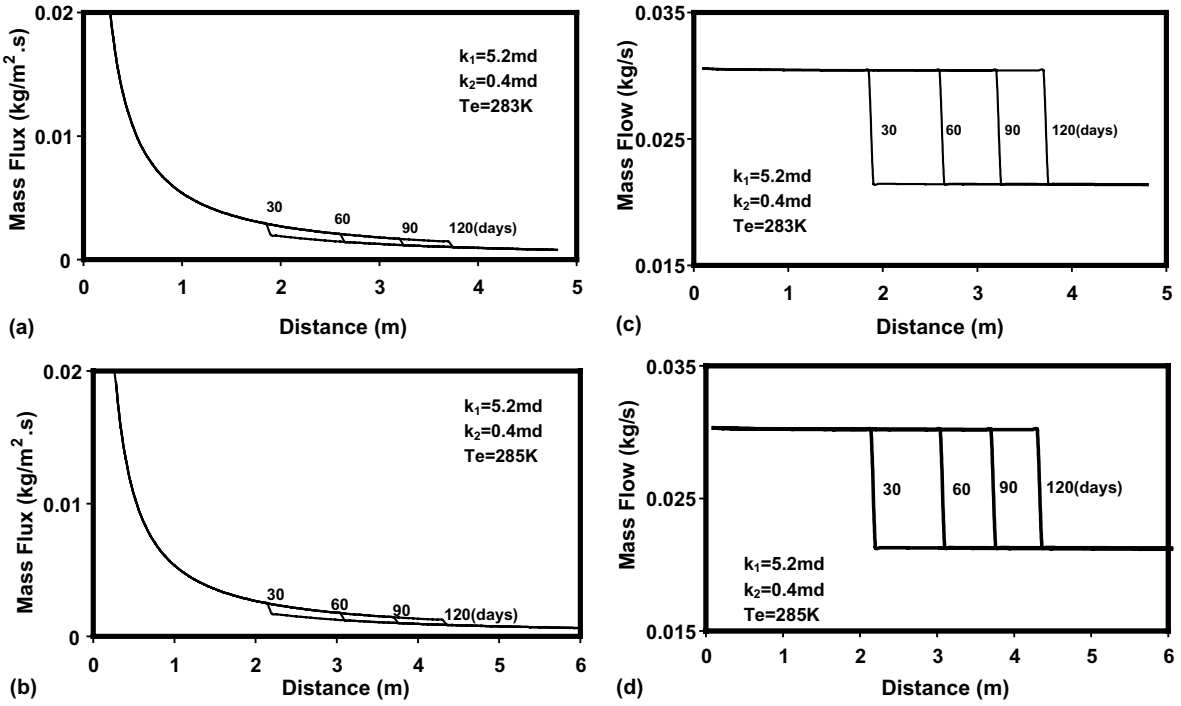

Fig. 10. Mass flux and mass flow profiles for a reservoir pressure of 15 MPa and a well natural gas output of 0.03 kg/s with different reservoir temperatures.

output is 0.04 kg/s is studied. Fig. 11a and b show the profiles for the case, that the permeabilities in the gas and hydrate zones are both 1 md. In this case the temperature has a smooth decreasing trend in the hydrate zone and decreases with a sharper slope in the gas zone. The pressure shows a gradual reduction in the entire reservoir but with a sharper slope in the gas zone. Similar to the one dimensional case reported by Ji et al. [6], it is rather difficult to identify the change in slope in the pressure profile at the front when the zone permeabilities are equal.

Fig. 11c and d show the profiles when the permeability in the gas zone is 5.2 md and the hydrate zone permeability is 1 md. In this case, there is an obvious pressure gradient change at the dissociation front. From Eq. (5), we expect that the gas flow out of the dissociation front into the gas zone should be larger than the gas flow into the front from hydrate zone, while at the dissociation front, the pressure gradient at the hydrate side is larger than that at the gas side. The difference in the zone permeability compensates, and the flow rate is larger on the gas side.

Fig. 12 shows the effect of gas zone permeability on the mass flux and total mass flow profiles. The reservoir conditions are identical to those for Fig. 11. Comparing Fig. 12a and b and Fig. 12c and d indicates that the variation of gas zone permeability has little effect on the mass flux and total mass flow profiles, respectively, as well as the location of the dissociation front. This observation shows that the variation of gas zone permeability only affects the reservoir temperature and pressure profiles, and its effect on hydrate dissociation at the decomposition front is slight.

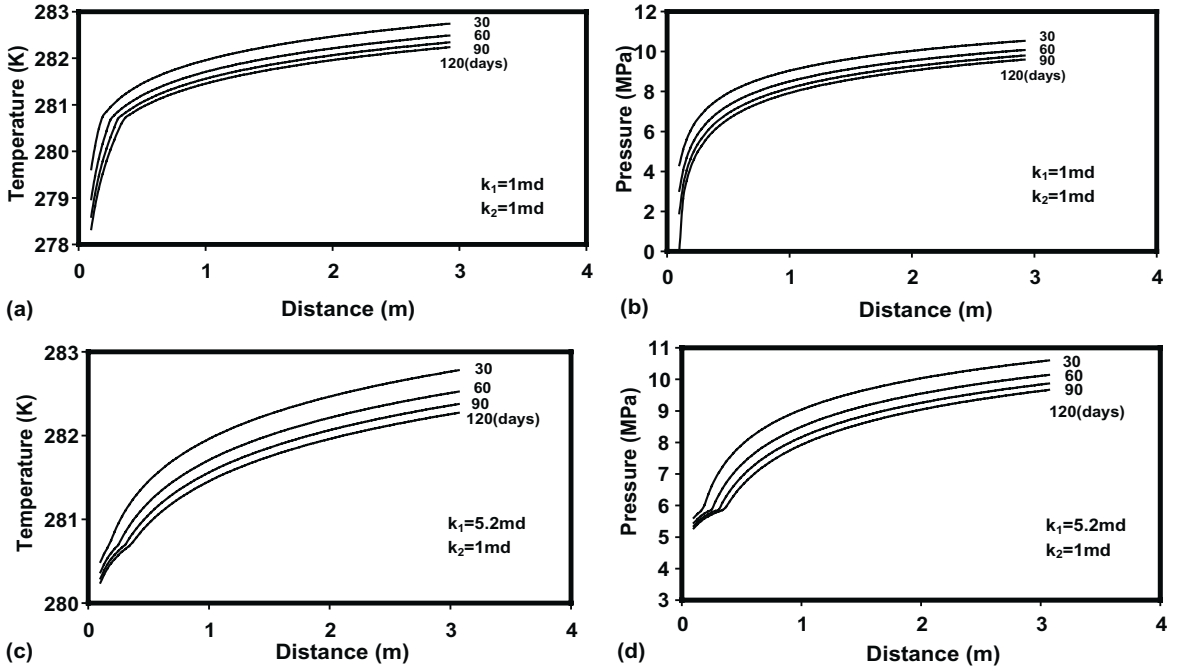

Fig. 11. Time variations of pressure and temperature profiles for a reservoir temperature of 287 K and a well natural gas output of 0.04 kg/s with different permeabilities.

Comparing Figs. 3 and 12 shows that the hydrate zone permeability significantly affects the natural gas total mass flow profiles. For $k_2 = 0.4$ md, the front is at 15 m after 90 days, while for a reservoir with $k_2 = 1$ md, the dissociation front is at about 0.5 m from the well. That is, at a constant well mass flow rate, a smaller k_2 will lead to a faster penetration of the front into the reservoir. This is because more hydrate needs to be dissociated to compensate for the lower gas flow rate in the hydrate zone.

Fig. 13 shows the movement of the dissociation front for different natural gas outputs. Here, the reservoir conditions are assumed to be fixed at 15 MPa and 287 K. The permeabilities in the gas and hydrate zones are, respectively, 5.2 and 0.4 md. Fig. 13 shows that the distance of the front from the well increases proportionally to the square root of time. As the natural gas output increases, the outward motion of the front increases.

For a fixed reservoir pressure and a natural gas output of 0.03 kg/s, the time evolutions of the dissociation front for different reservoir temperatures are shown in Fig. 14. It is observed that at the higher reservoir temperature, the dissociation front moves away from the well at a faster speed. At a fixed flow rate, a higher reservoir temperature leads to a higher level of hydrate dissociation that causes a more rapid motion of the front.

Fig. 15 shows the time evolutions of the dissociation front for different hydrate zone permeabilities for a natural gas output of 0.04 kg/s. Here, the reservoir pressure and temperature are, respectively, 15 MPa and 287 K. This figure shows that the dissociation front moves faster as the hydrate zone permeability decreases. As noted before, this is because at smaller hydrate zone

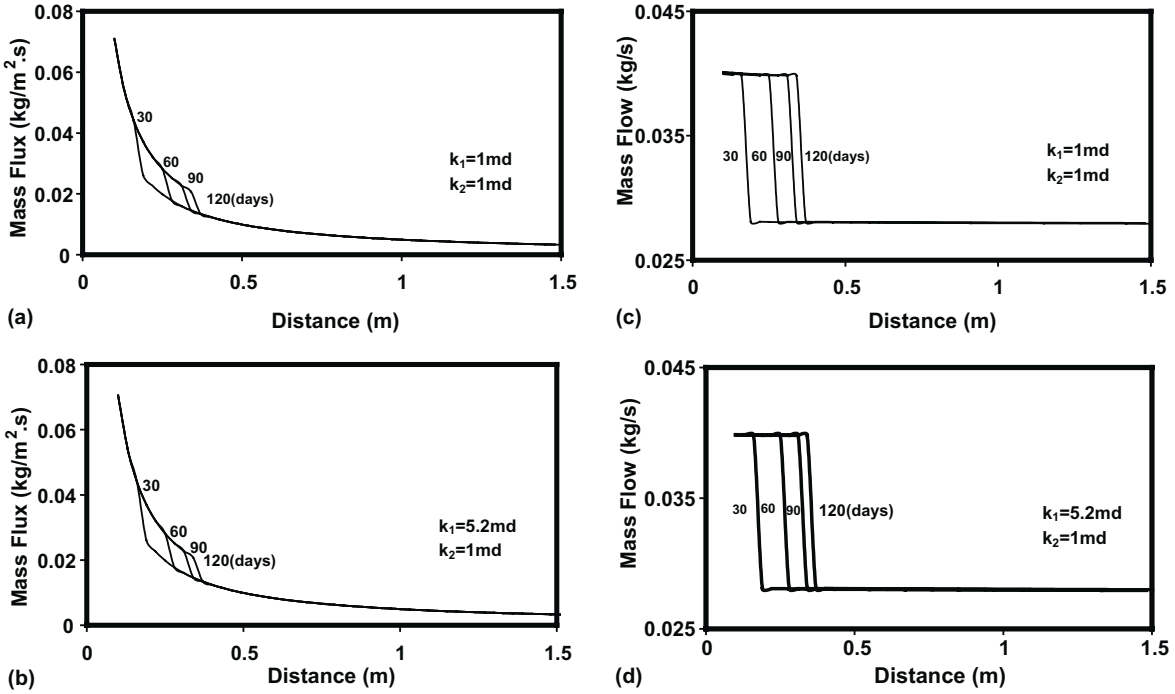

Fig. 12. Mass flux and mass flow profiles for a reservoir temperature of 287 K and a well natural gas output of 0.04 kg/s with different permeabilities.

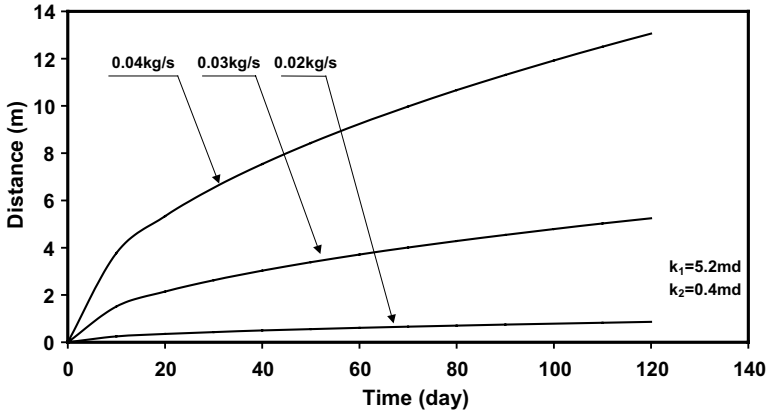

Fig. 13. Variations of the location of dissociation front for different well natural gas outputs.

permeability, the natural gas flow toward the front decreases. To maintain a fixed flow rate, a large amount of hydrate has to dissociate to compensate, and therefore, the dissociation front moves faster.

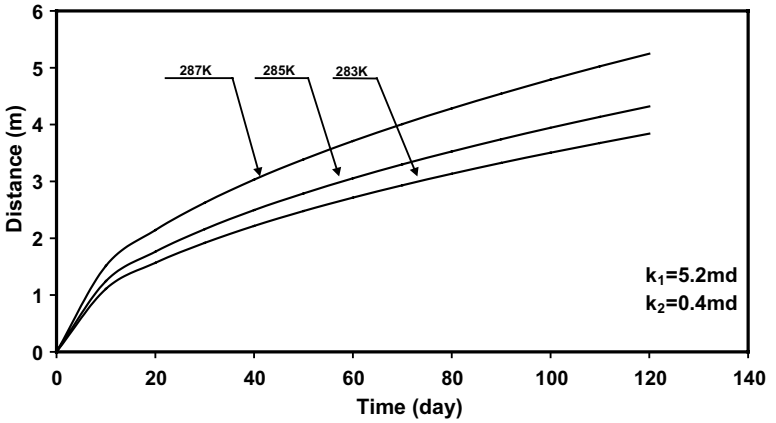

Fig. 14. Variations of the location of dissociation front for different reservoir temperatures for a well natural gas output of 0.03 kg/s.

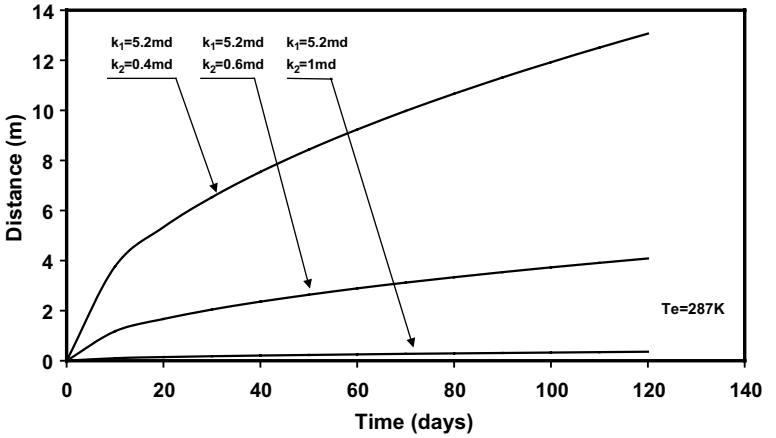

Fig. 15. Variations of the location of dissociation front for a well natural gas output of 0.04 kg/s and different permeabilities.

6. Conclusions

Dissociation of methane hydrate in confined, pressurized reservoirs for fixed well outputs is studied. Evolutions of pressure, temperature, mass flux and mass flow rate profiles in axisymmetric reservoirs under various conditions are analyzed. The effects of variation in well output, reservoir temperature and reservoir zone permeabilities are studied. On the basis of the results presented, the following conclusions may be drawn:

1. Under favorable conditions, natural gas can be produced at a fixed rate from hydrate reservoirs by a depressurization well.

2. For a large homogenous hydrate reservoir containing free natural gas, the dissociation pressure and temperature are fixed and depend only on the reservoir conditions and the well output.
3. For fixed reservoir pressure and temperature and a constant well production rate, the well pressure decreases with time. Thus, to maintain a constant natural gas output, the well pressure needs to be continuously reduced.
4. At low well output, the decrease in the well pressure is very slight. At high well outputs, the well pressure decreases rather quickly, and constant output can only be maintained for a short period of time.
5. The reservoir permeability in the hydrate zone significantly affects the natural gas production process.
6. For a fixed natural gas output, the pressure and temperature profiles have a smooth variation in the hydrate zone but have a sharper slope in the gas zone.
7. The gas mass flow rates in the hydrate and in the gas zone are roughly constant, with a sharp jump at the dissociation front.

As noted before, the presented linearization approach neglects the heat conduction in the reservoir and cannot enforce the balance of energy at the dissociation front. When this limitation is removed, the similarity solutions do not hold and the original nonlinear governing equations must be solved numerically. Such a study is currently being performed and the results will be reported in the near future.

Acknowledgements

The supports of the Office of Fossil Energy, US Department of Energy and Clarkson University are gratefully acknowledged. The work of GA was also supported by a grant from the US Department of Energy.

References

[1] AGU, American Geophysical Union, Mineralogical Society of America and Geochemical Society Spring Meeting, Boston, MA, June 1–4, 1999.
[2] Ahmadi G, Ji C, Smith DH. A simple model for natural gas production from hydrate decomposition. In: Proceedings of 3rd International Conference on Natural Gas Hydrates, Salt Lake City, UT, July 18–22, 1999.
[3] Burshears M. O'Brien TJ, Malone RD. A multi-phase, multi-dimensional, variable composition simulation of gas production from a conventional gas reservoir in contact with hydrates. In: Proceedings of Unconventional Gas Technology Symposium, Louisville, KY, May 18–21, Society of Petroleum Engineers, SPE 15246, 1986.
[4] Durgut I, Parlaktuna M. A numerical method for the gas production process in gas hydrate reservoirs. In: Proceedings of 2nd International Conference on Natural Gas Hydrates, Toulouse, France, June 2–6, 1996.
[5] Holder GD, Angert PF, Godbole SP. Simulation of gas production from a reservoir containing both gas hydrates and free natural gas. In: Proceedings of 57th Society of Petroleum Engineers Technology Conference, New Orleans, September 26–29, SPE11005, 1982.
[6] Ji C, Ahmadi G, Smith D. Natural gas production from hydrate decomposition by depressurization. Chem Eng Sci 2000;56:5801–14.

[7] Kamath V. Study of heat transfer characteristics during dissociation of gas hydrates in porous media. PhD Thesis, University of Pittsburgh, Pittsburgh, PA, 1983.
[8] Kim HC, Bishnoi PR, Heidemann RA, Rizvi SSH. Kinetics of methane hydrate decomposition. Chem Eng Sci 1987;42:1645–53.
[9] Lysne D. Hydrate plug dissociation by pressure reduction. In: Sloan Jr ED, Happel J, Hnatow MA, editors. International Conference on Natural Gas Hydrates, vol. 715. NY Academy of Sciences; 1993. p. 714–7.
[10] Makogon YF. Specialties of exploitation of the natural gas fields in permafrost conditions. Moscow: TsNTI Migazprom; 1966.
[11] Makogon YF. Hydrates of hydrocarbons. Tulsa, OK: Penn Well; 1997.
[12] Marshall DR, Saito S, Kobayashi R. AIChE J 1964;10:202.
[13] Masuda Y, Fujinaga Y, Naganawa S, Fujita K, Sato K, Hayashi Y. Modeling and experimental studies on dissociation of methane gas hydrates in Berea Sandstone Cores. In: Proceedings of 3rd International Conference on Natural Gas Hydrates, Salt Lake City, UT, July 18–22, 1999.
[14] Moridis G, Apps J, Pruess K, Myer L. EOSHYDR: A TOUGH2 Module for CH_4-hydrate release and flow in the subsurface. LBNL-42386, Lawrence Berkeley National Laboratory, Berkeley, CA, September, 1998.
[15] Sloan Jr ED. Clathrate hydrates of natural gases. 2nd ed. New York: Marcel Dekker; 1998.
[16] Selim MS, Sloan ED. Heat and mass transfer during the dissociation of hydrates in porous media. AIChE J 1989;35:1049–52.
[17] Tsypkin G. Mathematical models of gas hydrates dissociation in porous media. In: Proceedings of 3rd International Conference on Natural Gas Hydrates, Salt Lake City, UT, July 18–22, 1999.
[18] Verigin NN, Khabibullin IL, Khalikov GA. Izv Akad Nauk SSSr, Mekhanika Zhidkosti Gaza 1980;(1):174.